1.0

4.5
5.0
5.6
6.3

2.8   2.5

3.2

3.6

4.0

2.2

2.0

1.1

1.8

1.25   1.4   1.6

MICROCOPY RESOLUTION TEST CHART

NATIONAL BUREAU OF STANDARDS-1963-A

SECURITY CLASSIFICATION OF THIS PAGE (When Data Entered)

REPORT DOCUMENTATION PAGE

READ INSTRUCTIONS
BEFORE COMPLETING FORM

1. REPORT NUMBER	2. GOVT ACCESSION NO.	3. RECIPIENT'S CATALOG NUMBER
AFGL-TR-79-0217		

4. TITLE (and Subtitle)

CHARGING ANALYSIS OF THE SCATHA SATELLITE

5. TYPE OF REPORT & PERIOD COVERED

Scientific. Interim.

6. PERFORMING ORG. REPORT NUMBER

7. AUTHOR(s)

G. W. Schnuelle*   M. J. Mandell*
D. E. Parks*   P. G. Steen*
I. Katz*   J. J. Cassidy*
                      A. Rubin

8. CONTRACT OR GRANT NUMBER(s)

9. PERFORMING ORGANIZATION NAME AND ADDRESS

Air Force Geophysics Laboratory (PHG)
Hanscom AFB
Massachusetts 01731

10. PROGRAM ELEMENT, PROJECT, TASK AREA & WORK UNIT NUMBERS

7661

11. CONTROLLING OFFICE NAME AND ADDRESS

Air Force Geophysics Laboratory (PHG)
Hanscom AFB
Massachusetts 01731

12. REPORT DATE

27 September 1979

13. NUMBER OF PAGES

21

14. MONITORING AGENCY NAME & ADDRESS(if different from Controlling Office)

15. SECURITY CLASS. (of this report)

Unclassified

15a. DECLASSIFICATION DOWNGRADING SCHEDULE

16. DISTRIBUTION STATEMENT (of this Report)

Approved for public release; distribution unlimited.

Scientific interim rept.,

17. DISTRIBUTION STATEMENT (of the abstract entered in Block 20, if different from Report)

NAS3-21050

18. SUPPLEMENTARY NOTES Published in NASA Conference Publ. 2071 -
AFGL-TR-79-0082, 1979 Presented at USAF/NASA Spacecraft Charging
Technology Conference, USAF Academy, Colorado 31 Oct-2 Nov 78
*Systems, Science and Software

19. KEY WORDS (Continue on reverse side if necessary and identify by block number)

NASCAP
SCATHA model
Spacecraft charging theory

20. ABSTRACT (Continue on reverse side if necessary and identify by block number)

We describe here a detailed model of the geometrical, material, and
electrical properties of the SCATHA satellite for use with the NASA Charging
Analyzer Program (NASCAP). Charging calculations in an intense magneto-
spheric substorm environment demonstrate that: (1) long booms can
significantly perturb the potentials near the spacecraft, and (2) discharging
by sunlight or by active control can cause serious time-dependent
differential charging problems.

DD FORM 1473 EDITION OF 1 NOV 65 IS OBSOLETE
1 JAN 73

390 310

SYSTEMS, SCIENCE AND SOFTWARE

38 507

CHARGING ANALYSIS OF THE SCATHA SATELLITE

G. W. Schnuelle, D. E. Parks, I. Katz,
M. J. Mandell, P. G. Steen, J. J. Cassidy
Systems, Science and Software

A. Rubin
Air Force Geophysics Laboratory

Presented at

USAF/NASA SPACECRAFT CHARGING TECHNOLOGY CONFERENCE

U.S. AIR FORCE ACADEMY, COLORADO

31 October — 2 November 1978

DDC

OCT 11 1979

A

CHARGING ANALYSIS OF THE SCATHA SATELLITE

G. W. Schnuelle, D. E. Parks, I. Katz,
M. J. Mandell, P. G. Steen, J. J. Cassidy
Systems, Science and Software

A. Rubin
Air Force Geophysics Laboratory

ABSTRACT

We describe here a detailed model of the geometrical, mate-
rial, and electrical properties of the SCATHA satellite for use
with the NASA Charging Analyzer Program (NASCAP). Charging cal-
culations in an intense magnetospheric substorm environment demon-
strate that: (1) long booms can significantly perturb the poten-
tials near the spacecraft, and (2) discharging by sunlight or by
active control can cause serious time-dependent differential
charging problems.

1. INTRODUCTION

We have developed a detailed model of the SCATHA satellite
for use with the NASA Charging Analyzer Program (NASCAP) (refs.
1 and 2). The model accounts for such geometrical complexities
as booms, shadowing, and the presence of insulating materials
over portions of the conducting ground of the space vehicle. The
effects of photoemission and secondary emission caused by electron
and ion impact, active control devices such as electron and ion
beams, and surface and bulk conductivity are included in the
model. To our knowledge, this model represents the most complete
and realistic treatment of spacecraft charging attempted to date
for any satellite.

Section 2 below describes the SCATHA model employed in
NASCAP. A detailed shadowing study was performed for a geometri-
cally more accurate SCATHA model; this work is described in Sec-
tion 3. We have performed charging calculations for one environ-
ment using the present model, and the results of these calcula-
tions are described in Section 4. Preliminary conclusions of this
study are summarized in Section 5.

1

2. SCATHA MODEL DEVELOPMENT

The NASCAP program allows the specification of the geometrical, material, and electrical properties of a spacecraft in considerable detail. We have attempted to incorporate the most current and complete information available for SCATHA into our model. However, the present model is meant primarily to illustrate the intended level and scope of our study, rather than to provide the final word on a model specification. The NASCAP code allows model features to be easily altered to make our model a more faithful representation of the SCATHA satellite if the need arises.

Perspective views of our gridded model are shown in figures 1 and 2. The main body of the satellite is represented as a right octagonal cylinder, with the aft cavity visible in figure 2. The OMNI antenna and the SC9 cluster of experiments are visible on the forward surface of the satellite. Our model reproduces the actual SCATHA geometrical features extremely well, as shown in table 1. Note in particular that the treatment of booms in NASCAP allows the actual boom radii to be reproduced exactly in the model. The requirements in NASCAP that booms parallel coordinate axes and intercept mesh points in all grids effectively force any long booms to pass through the center of the innermost mesh. Therefore, our present model includes only the SC6, SC11, and the two SC2 booms, with the orientations fixed at right angles to one another.

Figure 3 illustrates the computational space in which NASCAP solves Poisson's equation for this model. Monopole boundary conditions are imposed on the edges of the outermost grid, which is a rectangular prism of dimensions 1.6 × 1.6 × 3.2 m. The zone size decreases by a factor of 2 in each of the four successive inner grids, so that the effective resolution is 11.5 cm near the satellite body. (Local mesh refinement techniques in NASCAP allow a resolution of 2.5 cm for selected zones on the satellite.)

Our model includes the specification of 15 distinct exposed surface materials, each of which is specified by the values of some 13 user-supplied parameters. The surface materials are described in table 2. We have attempted to find experimentally measured values for all parameters; where this has not been possible, suitable estimates based on the properties of similar materials have been used. Table 3 lists the values employed in the calculations reported here. The analytical expressions in which these parameters are used to evaluate net surface currents are described in detail in reference 5. The formulation of electron backscattering in NASCAP has been somewhat modified recently, and the newer treatment is described in appendix A. The exposed materials are illustrated in figure 4 in which the locations of several of the SCATHA experiments are also shown. Experiments at the ends of SCATHA booms are modeled as a single boom segment

2

whose radius is adjusted to match the exposed surface area of the actual experiment.

The model includes six distinct underlying conductors: spacecraft ground, the reference band, and the four experiments SC2-1, SC2-2, SC6-1 and SC6-2. Each of these underlying conductors is capacitively coupled to spacecraft ground, and each can be separately biased with respect to ground. A seventh conductor could be introduced to underlay the solar cells at an appropriate bias. In this study the reference band was allowed to float and all other conductors were biased to the ground potential.

NASCAP has extensive capabilities to model particle emitters and detectors located on the spacecraft body, as described previously (ref. 2). These features of NASCAP can be used in the analysis of the operation of, for example, the SCATHA experiments SC4, SC5, SC6, SC7, and SC9. Such studies should be particularly helpful in determining the influence of spacecraft fields on particles emitted during active control, and in determining the source of particles seen at detector sites.

3. SHADOWING STUDY

For the SCATHA shadowing study, we were required to generate percent shadowing tables for various experiments. We were able to generate accurate tables using relatively small amounts of computer time: less than 5 minutes Univac 1100/81 time was required for a table of 7560 entries.

Since the geometrical capabilities of the NASCAP shadowing routines are more general than the rest of the code, we were able to employ a SCATHA model for shadowing in which each experiment was treated geometrically in much finer detail than in the model described in Section 2. Figure 5 shows the level of detail in a perspective view of the ML12-7 experiments on the forward surface. Booms were placed at their actual locations on the satellite, and the experiments at the boom ends were given a great deal of geometrical complexity. Figure 6 shows the SC2-1, SC1-4, and SC6-1 booms as they were resolved in the shadowing study.

These detailed geometrical shapes were input to the usual NASCAP shadowing routines (HIDCEL) for table generation. The tables cover satellite rotation in 1° increments for the satellite plane deviations from the sun line of -5° to +5°.

4. CHARGING CALCULATIONS

The model was subjected to an extremely intense substorm described by a superposition of two Maxwellian plasmas with the following parameters:

$$\theta_{e1} = 40,000 \text{ eV} \qquad\qquad \theta_{e2} = 100 \text{ eV}$$

$$\theta_{i1} = 20,000 \text{ eV} \qquad\qquad \theta_{i2} = 100 \text{ eV}$$

$$n_{e1} = 10 \text{ cm}^{-3} \qquad\qquad n_{e2} = 10 \text{ cm}^{-3}$$

$$n_{i1} = 10 \text{ cm}^{-3} \qquad\qquad n_{i2} = 10 \text{ cm}^{-3}$$

The effects of ambient space charge were neglected in the solution of Poisson's equation here, since the mean satellite radius, r_s, is much smaller than the plasma Debye length, λ_D.

$$r_s \sim 100 \text{ cm}$$

$$\lambda_D \sim 700 \sqrt{\frac{\theta}{n_e}} \sim 2200 \text{ cm}$$

$$r_s/\lambda_D \sim 0.05$$

There was no sunlight present in the first calculation described below.

Potential contours during the initial overall charging phase ($\sim 10^{-3}$ seconds) are shown in figures 7 and 8. The question of whether booms have a significant effect on the sheath potentials is clearly answered by examining figure 9, which shows potential contours in a plane a half meter below the plane of the booms. Figure 10 shows similar contours in a calculation with the booms omitted; the distortion of contours by the booms is obvious. While the boom radii are small, ~ 2 cm, the effect on potentials is related to the boom capacitance, which varies only logarithmically with radius. This results in long range potential interactions from thin booms, where the characteristic decay distance is closer to the boom length than to the boom radius.

The rapid initial charging is followed by a much slower development of differential charging, as illustrated in figure 11. For this example the maximum differential developed after 22 seconds was 700 volts and the maximum field strength in a dielectric layer was 24,000 volts/cm. Figure 12 shows contours in the plane of the booms after 22 seconds; note the differential charging developed at the boom ends due to variations in the material properties between the experiments and the boom coatings.

The two Maxwellian description of the plasma leads to a low overall charging voltage of only -7.3 keV despite the presence of a plasma component with an electron temperature of 40 keV. For the particular case we have studied here, low energy protons are being collected at an enormous rate and these, augmented by the secondary electrons they produce, balance the incident electron current. NASCAP uses a proton collection model in which the collection increases linearly with voltage, which is valid in the present case where r_s/λ_D is small, as discussed by Laframboise (ref. 4). Table 4 shows the detailed current balance near equilibrium for the boom surface material in the presence of the double Maxwellian environment described above. Also shown in table 4 is a similar breakdown for the same material subjected only to the high energy single Maxwellian component. The equilibrium potential is -32 keV in this case, indicating that the final potentials reached would have been much lower had we employed a single Maxwellian plasma model. For both plasma models, the final potentials reached will depend on the exact values employed for the proton and electron induced secondary yields. Great care should be exercised in the determination of the values and associated error estimates for parameters which affect the production of secondary electrons in these and similar calculations.

Finally, the atomic number dependence of backscatter coefficients tends to make high-Z materials charge less negatively than other elements. For SCATHA, this means that the magnitude of the boom potentials will be significantly lower than most other surfaces, since exposed platinum constitutes much of its surface area.

We have performed a similar calculation on this model in which the sunlight was turned on after 22 seconds of charging in eclipse. The photoemission results in strong differential charging ($\sim$3 keV) along the booms, as shown in figure 13. In our model the boom surfaces are very weakly capacitively coupled to the grounded cable shields which extend the length of the booms, while the experiments at the ends of the SC2 and SC6 booms are coupled closely to spacecraft ground. This weak coupling has the effect of allowing the booms to react rapidly to environmental perturbations compared to the rest of the satellite, leading to temporary conditions of high differential charging. We have observed similar effects when discharging the satellite with an electron gun.

The potentials near the satellite in sunlight are dominated by the monopole field of the spacecraft body. A photoemitting boom surface element can discharge only to the value of the local monopole potential, since further discharge is limited by immediate reflection of photoelectrons. This has the amazing consequence that the booms, strongly perturbing in eclipse, now seem to disappear in the potential contours near the satellite body. Note that significant differential charging in sunlight along the

5

SC2 booms will certainly persist at equilibrium due to large differences between the photoemission from surfaces on booms and on the SC2-1 and SC2-2 experiments. Our calculations neglect any effective surface conductivity parallel to the booms due to the presence of a photosheath. The surface conductivity features of NASCAP could easily be invoked to simulate this effect, which would reduce the magnitude of the differential charging observed here.

The calculations reported here were performed on the Univac 1100/81 computer at Systems, Science and Software. Each cycle of charging and solution of the potential equations required approximately 15 minutes CPU time during differential charging, and 5 minutes CPU time when no differential charging occurred. Approximately 10 cycles of each type were required for the calculations reported here. We have developed a second SCATHA model for testing purposes in which the zone size is twice that of the model presented here and the booms are shortened; computer times are reduced by roughly 80 percent for this model, and all of the results described above can be observed in calculations using the smaller model. The half-scale model will be useful whenever fine resolution on the satellite surfaces is not required.

5. CONCLUSIONS

We have completed the development of a detailed model of the SCATHA satellite. Preliminary results from calculations in one magnetospheric environment indicate that:

- The presence of a low energy component in a two Maxwellian description of the magnetospheric environment reduces the maximum charging of a satellite relative to that found for a single Maxwellian.

- The booms have substantial impact on potentials near the spacecraft in eclipse.

- The use of high atomic number coatings, such as platinum on the booms, may increase the severity of differential charging.

- Discharging by sunlight or by active control may lead to transient increases in differential charging along the booms due to the weak coupling of the booms to spacecraft ground.

Our calculations demonstrate that the prediction of spacecraft potentials for SCATHA is an exceedingly complex problem, in which the full capabilities of the NASCAP treatment of geometrical features, material properties, and dynamic interaction with the environment are utilized. We plan to continue this study of

6

SCATHA using NASCAP with particular emphasis on boom perturbations and the effects of active control.

APPENDIX A.   ELECTRON BACKSCATTER

Electron backscatter is modeled in NASCAP as a function of electron energy and mean atomic number of backscattering material. The formulation first used in NASCAP (ref. 5) was valid only for low Z-materials. To remove this restriction we have used a formula of Burke (ref. 6) to obtain the backscatter coefficient for isotropically incident electrons as

$$\eta_1 = 0.475 \ z^{0.177} - 0.40 \ . \tag{A1}$$

The backscatter coefficient for normal incidence, η_o, is then found by solving the equation

$$\eta_1 = 2[1 - \eta_o(1 - \ln \eta_o)]/(\ln \eta_o)^2 \tag{A2}$$

which comes from assuming the angular dependent backscatter coefficient (ref. 7) to be

$$\eta(\theta) = \eta_o \exp[-(\ln \eta_o) \ (1 - \cos\theta)] \ . \tag{A3}$$

The energy dependence (ref. 4) is then taken to be

$$\eta_o(\varepsilon) = \gamma(\varepsilon) \ (\eta_o + 0.1 \ \exp(-\varepsilon/5)) \tag{A4}$$

$$\gamma(\varepsilon) = \begin{cases} 0 & \varepsilon < 50 \text{ eV} \\ \ln \ (20 \ \varepsilon)/\ln 20 & 50 \text{ eV} < \varepsilon < 1 \text{ keV} \\ 1 & \varepsilon > 1 \text{ keV} \end{cases}$$

where ε is in keV.

The energy dependent η_o from (A4) is then used in (A2) or (A3) to calculate the relevant backscatter coefficient.

REFERENCES

1. Katz, I., Parks, D. E., Mandell, M. J., Harvey, J. M. and Wang, S. S., "NASCAP, A Three-Dimensional Charging Analyzer Program for Complex Spacecraft," IEEE Transactions on Nuclear Science, 6, 1977, p. 2276.

2. Katz, I., Cassidy, J. J., Mandell, M. J., Schnuelle, G. W., Steen, P. G. and Roche, J. C., "The Capabilities of the NASA Charging Analyzer Program," preceding paper at this conference.

3. Steen, P. G., "SCATHA Experiment Shadowing Study," Systems, Science and Software Topical Report SSS-R-78-3658, May 1978.

4. Laframboise, J. G., UTIAS Report No. 100, 1966.

5. Katz, I., Parks, D. E., Mandell, M. J., Harvey, J. M., Brownell, Jr., D. H., Wang, S. S. and Rotenberg, M., "A Three-Dimensional Dynamic Study of Electrostatic Charging in Materials," NASA CR-135256, August 1977.

6. Burke, E. A., "Soft X-ray Induced Electron Emission," IEEE Transactions on Nuclear Science, NS-24, 1977, pp. 2505-2509.

7. Darlington, E. H. and Cosslett, V. E., "Backscattering of 0.5-10 keV Electrons from Solid Targets," J. Phys. D5, 1972, p. 1969.

TABLE 1.   COMPARISON OF ACTUAL SCATHA GEOMETRICAL FEATURES TO
          GRIDDED NASCAP MODEL

Zone Size = 4.54 in. (11.5 cm)

	SCATHA	MODEL
Radius	33.6 inches	32.0 inches
Height	68.7	68.0
Solar Array Height	29	27.2
Bellyband Height	11.3	13.6
SC9-1 Experiment	9.2 × 6 × 8	9.1 × 4.5 × 9.1
SC6-1 Boom	1.7 (radius)	1.7
	118 (length)	113.2
Surface Area	2.16×10^4 sq. in.	2.11×10^4 sq. in.
Solar Array Area	1.23×10^4	1.15×10^4
Forward Surface Area	0.36×10^4	0.34×10^4

TABLE 2. EXPOSED SURFACE MATERIALS

GOLD: gold plate

SOLAR: solar cells, coated fused silica

WHITEN: non-conducting white paint (STM K792)

SCREEN: SC5 screen material, a conducting fictitious
            material which absorbs but does not emit
            charged particles

YELOWC: conducting yellow paint

GOLDPD: 88 percent gold plate with 12 percent conductive
            black paint (STM K748) in a polka dot pattern

BLACKC: conductive black paint (STM K748)

KAPTON: kapton

SIO2:   SiO$_2$ fabric

TEFLON: teflon

INDOX: indium oxide

YGOLDC: conducting yellow paint (50 percent)
            gold (50 percent)

ML12:   ML12-3 and ML12-4 surface, a fictitious material
            whose properties are an average of the proper-
            ties of the several materials on the ML12 sur-
            faces

ALUM: aluminum plate

BOOMAT: platinum banded kapton

TABLE 3. MATERIAL PROPERTIES FOR EXPOSED SURFACES[a]

Property[b]	GOLD	SOLAR	WHITEN	SCREEN	BLACKC YELOWC	GOLDPD	KAPTON
1	-	4.00+00	3.50+00	-	3.50+00	-	3.50+00
2	1.00-03	1.79-04	5.00-05	1.00-03	5.00-05	1.00-03	1.25-04
3	∞	1.00-14	5.90-14	∞	5.00-10	∞	1.00-14
4	7.90+01	1.00+01	5.00+00	1.00+00	5.00+00	7.01+01	5.00+00
5	8.80-01	4.10+00	2.10+00	0.00	2.10+00	1.03+00	2.10+00
6	8.00-01	4.10-01	1.50-01	1.00+00	1.50-01	7.20-01	1.50-01
7	8.30+01	-1.00+00	-1.00+00	1.00+01	-1.00+00	8.30+01	-1.00+00
8	1.63+00	0.00	0.00	1.50+00	0.00	1.63+00	0.00
9	3.46+01	2.30+00	1.05+00	0.00	1.05+00	3.46+01	1.42+00
10	7.00-01	2.08+01	9.80+00	1.00+00	9.80+00	7.00-01	9.80+00
11	4.00-01	1.36+00	1.40+00	0.00	1.40+00	4.00-01	1.40+00
12	5.00+01	4.00+01	7.00+01	1.00+00	7.00+01	5.00+01	7.00+01
13	2.90-05	2.00-05	2.00-05	0.00	2.00-05	2.90-05	2.00-05

Property[b]	SIO2	TEFLON	INDOX	YGOLDC	ALUMIN	BOOMAT[c]	ML12
1	4.00+00	2.00+00	-	-	-	2.00+00	-
2	2.75-04	1.25-04	1.00-03	1.00-03	1.00-03	5.00-03	1.00-03
3	2.75-12	1.00-14	∞	∞	∞	1.00-10	∞
4	1.00+01	1.00+01	2.44+01	4.20+01	1.30+01	6.34+01	6.00+00
5	2.40+00	3.00+00	1.40+00	1.49+00	9.70-01	1.86+00	1.00+00
6	4.00-01	3.00-01	8.00-01	4.80-01	3.00-01	5.90-01	3.00-01
7	-1.00+00	-1.00+00	-1.00+00	-1.00+00	2.60+02	8.30+01	-1.00+00
8	0.00	0.00	0.00	-1.00+00	1.30+00	1.63+00	0.00
9	1.02+00	2.00+00	7.18+00	1.02+01	2.40+02	3.46+01	2.00+00
10	2.00+01	1.67+01	5.55+01	4.20+01	1.73+00	7.00-01	1.20+01
11	1.40+00	1.40+00	1.36+00	1.00+00	1.36+00	4.00-01	1.40+00
12	7.00+01	7.00+01	4.00+01	6.00+01	4.00+01	5.00+01	7.00+01
13	2.00-05	2.00-05	3.20-05	2.40-05	4.00-05	2.72-05	2.10-05

TABLE 3.   (Continued)

[a]The materials are described in Table 2.

[b]The thirteen properties are as follows (see Reference 4 and Appendix A for further details):

Property 1:	Relative dielectric constant for insulators (dimensionless).
Property 2:	Thickness of dielectric film or vacuum gap (meters).
Property 3:	Electrical conductivity (mho/m). The value ∞ indicates a vacuum gap over a conducting surface.
Property 4:	Atomic number (dimensionless).
Property 5:	Maximum secondary electron yield for electron impact at normal incidence (dimensionless).
Property 6:	Primary electron energy to produce maximum yield at normal incidence (keV).
Properties 7-10:	Range for incident electrons. Either:

$$Range = P_7E^{P_8} + P_9E^{P_{10}}$$

where the range is in angstroms and for the energy in keV,

<u>or</u>

$P_7 = -1.$ to indicate use of an empirical range formula

P_9 = density (g/cm^3)

P_{10} = mean atomic weight (dimensionless).

Property 11:	Secondary electron yield for normally incident 1 keV protons.
Property 12:	Proton energy to produce maximum secondary electron yield (keV).
Property 13:	Photoelectron yield for normally incident sunlight (A/m^2).

[c]The dielectric constant and thickness for the boom surfaces were chosen to reflect the <u>effective</u> capacitance to the underlying cable shield.

TABLE 4. COMPONENTS OF INCIDENT AND EMITTED CURRENTS (10^{-5} A/m^2) FOR BOOM SURFACE MATERIAL NEAR STEADY STATE.

	Double Maxwellian	Single Maxwellian
Potential	-7000 Volts	-32,000 Volts
Incident Electrons	-4.6	-2.3
Resulting Backscatter	2.7	1.4
Resulting Secondaries	.7	.4
Incident Protons	.6	.2
Resulting Secondaries	.6	.3
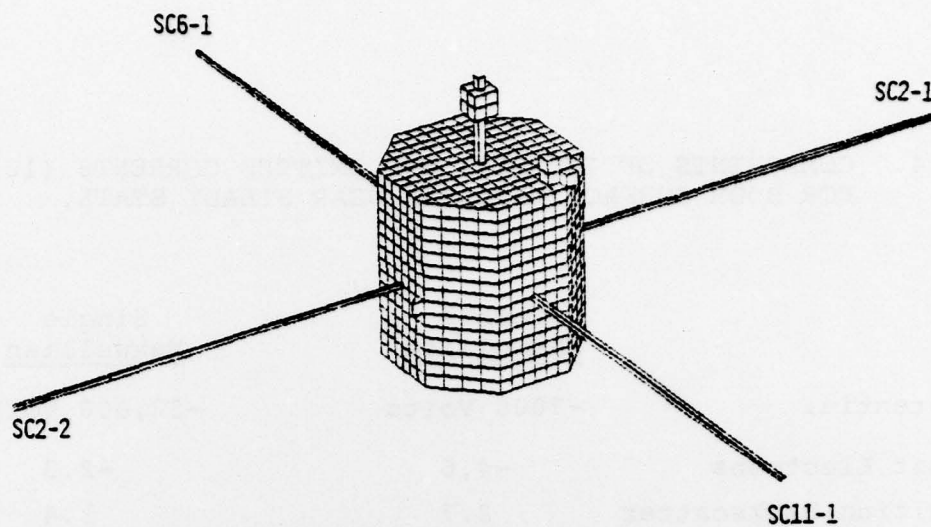
Figure 1. SCATHA model: side view. The 50 m antenna and the SC1-4 boom are not included in this model.
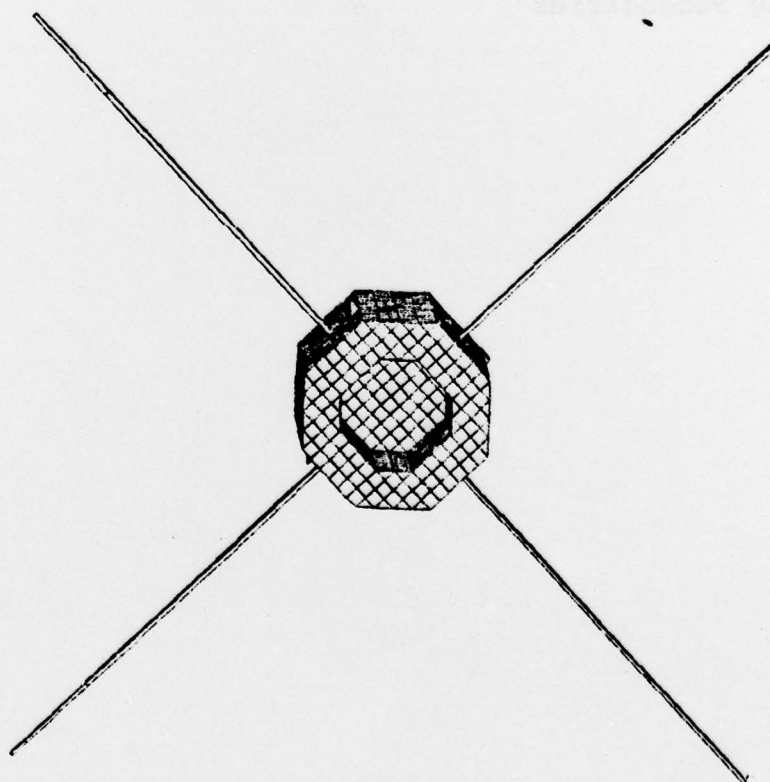
Figure 2. SCATHA model: bottom view with aft cavity visible.
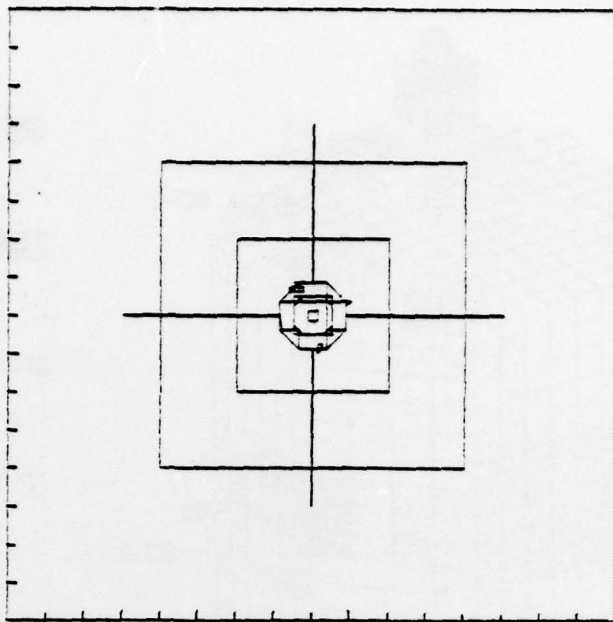
Figure 3. Computational space surrounding the SCATHA model, show-
ing the nesting of the grids. The tic marks along the axes indi-
cate the outer grid zone size; the zone size decreases by a factor
of two in successive grids.
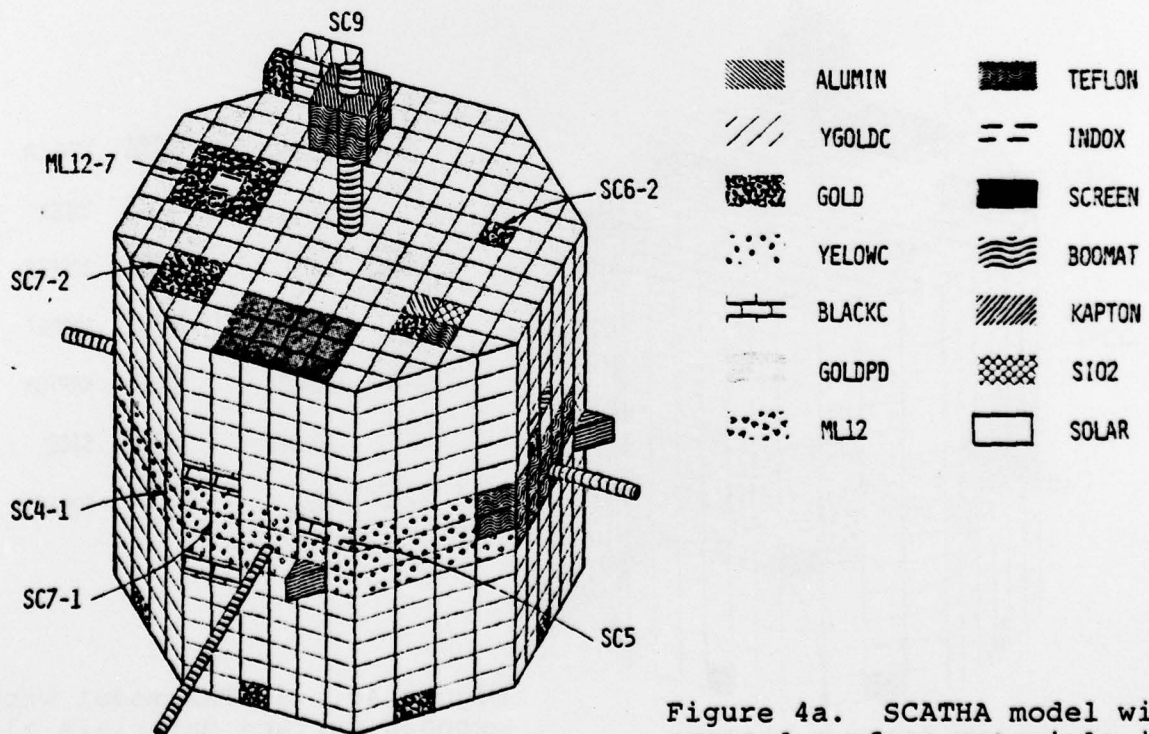
Figure 4a. SCATHA model with
exposed surface materials il-
lustrated.

15
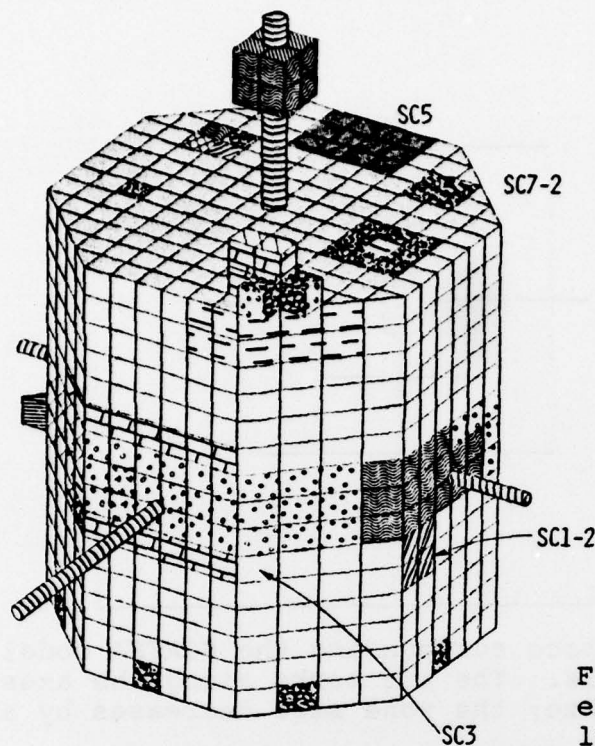
Figure 4b. SCATHA model with exposed surface materials illustrated.
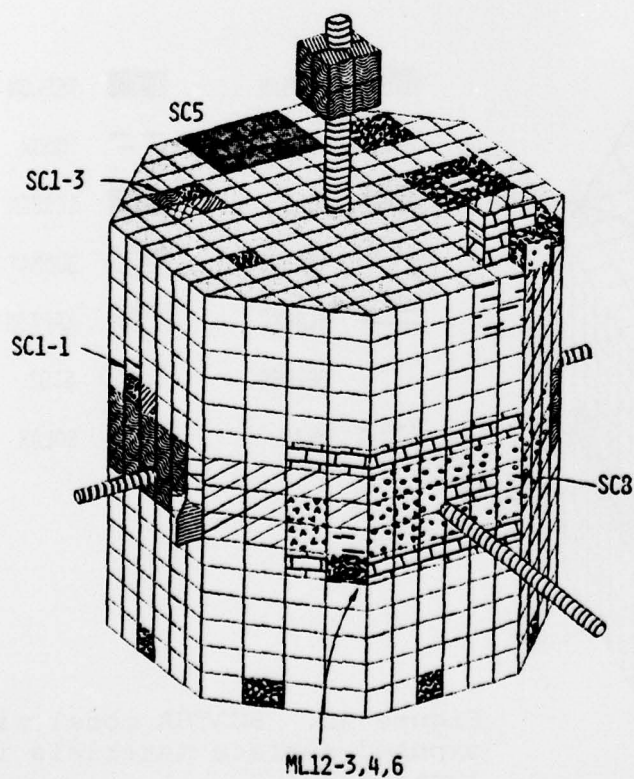
Figure 4c. SCATHA model with exposed surface materials illustrated.

16
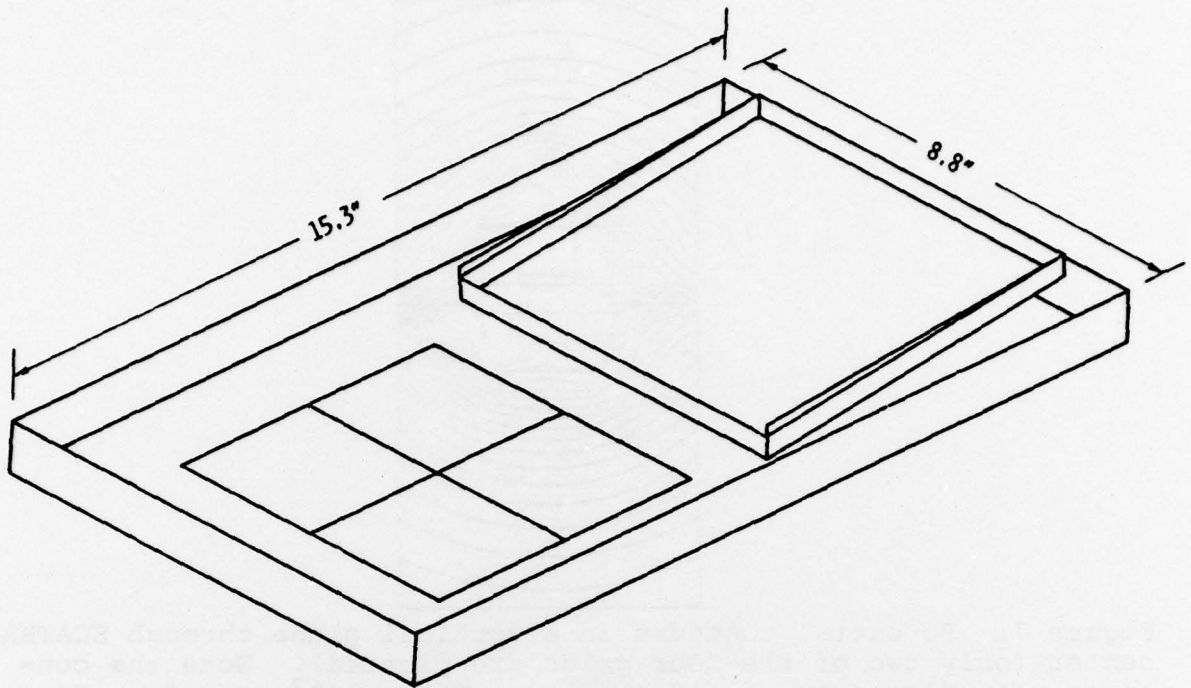
Figure 5. ML12-7 experiment as resolved for the SCATHA shadowing study.

SC2-1

SC1-4

SC6-1
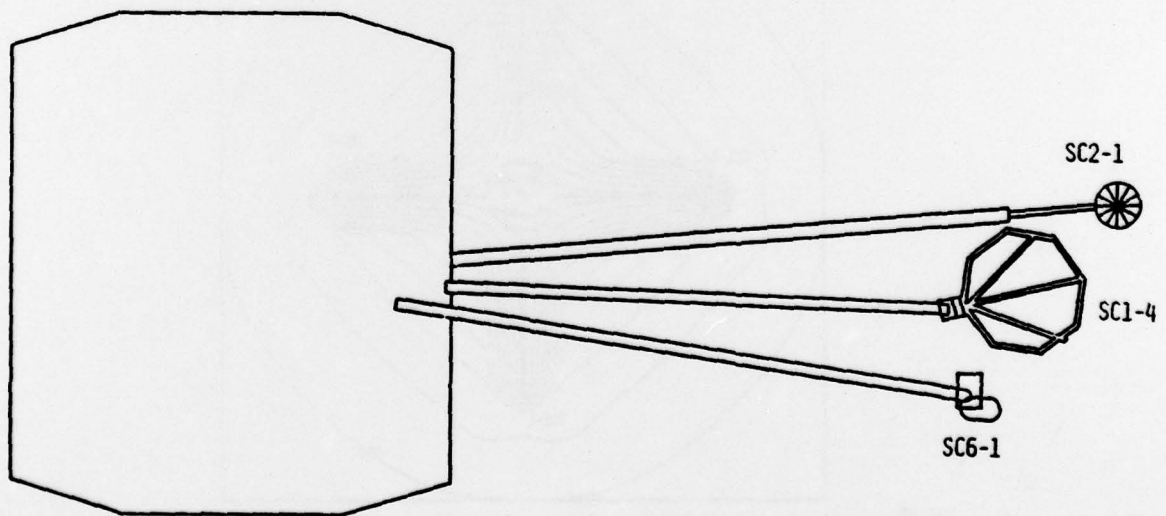
Figure 6. SCATHA booms as resolved in the shadowing study.

17
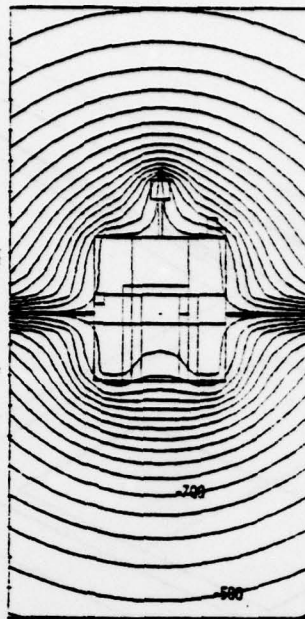
Figure 7. Potential contours in a vertical plane through SCATHA
center (only two of the four grids are plotted). Note the con-
tours extending into the aft cavity. Time $\sim 10^{-3}$ seconds. Con-
tours from -450 to -1250 volts in 50 volt steps.
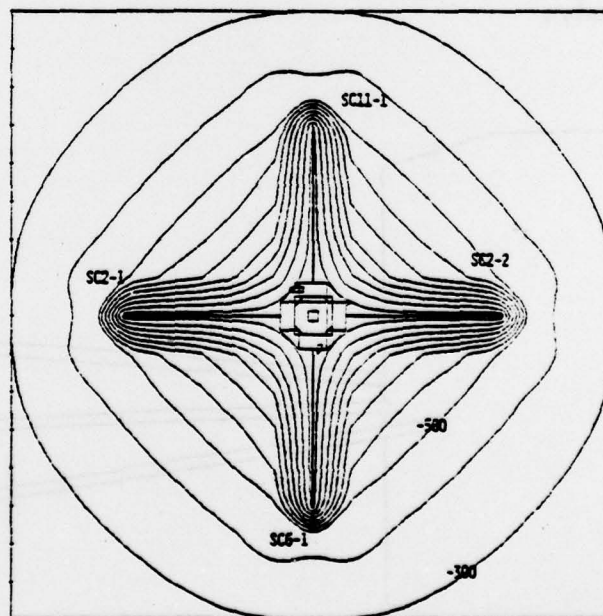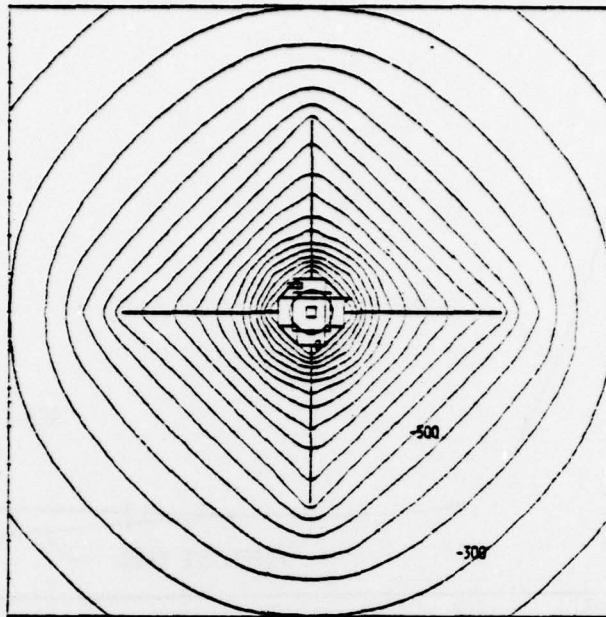

Figure 8. Potential contours in a horizontal plane through SCATHA
center. Time $\sim 10^{-3}$ seconds. Contours from -300 to -1200 volts in
100 volt steps. The relative orientations of the booms is the
same in later figures. The dimples in the potential contours
near the boom ends are artifacts associated with an imperfect
match of potential interpolation functions.

18

Figure 9. Potential contours in a horizontal plane 1 m below
SCATHA center. Time $\sim 10^{-3}$ seconds. Contours from -250 to -1150
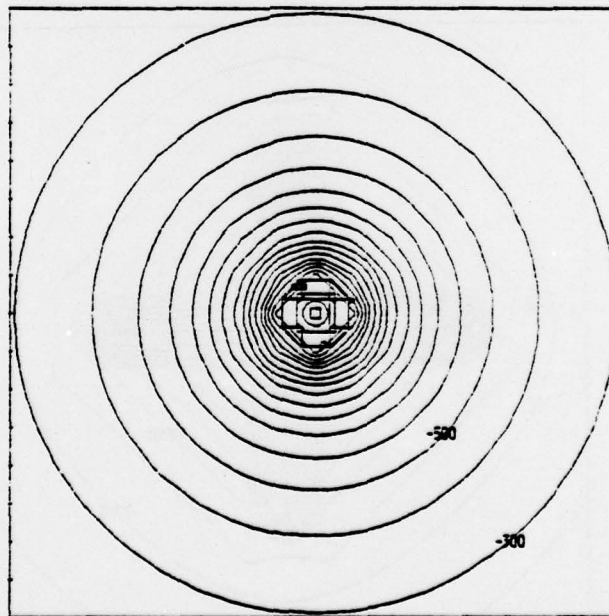volts in 50 volt steps.

Figure 10. Potential contours in a horizontal plane 1 m below
SCATHA center for a model in which the booms have been removed.
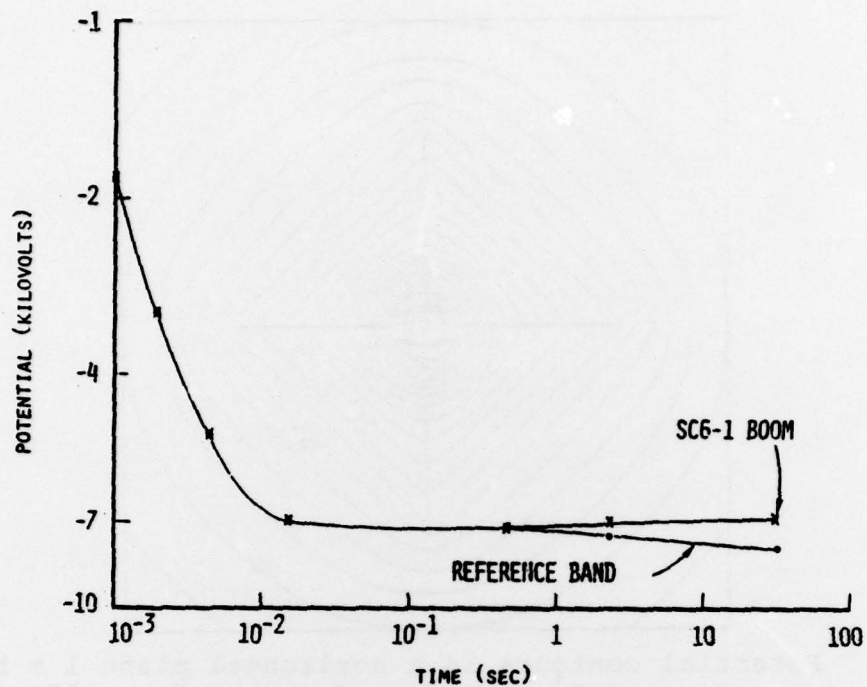Time $\sim 10^{-3}$ seconds. Contours from -300 to -1900 volts in 100
volt steps.

Figure 11. Spacecraft potential versus time for two points on SCATHA satellite.
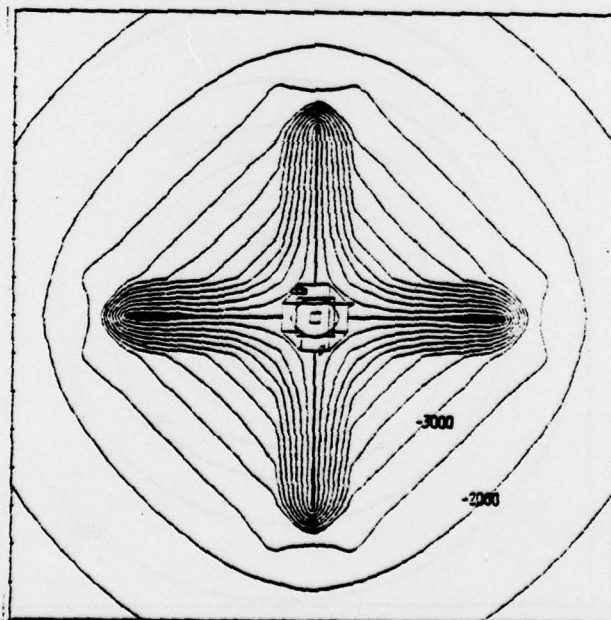

Figure 12. Potential contours in a horizontal plane through SCATHA center, with differential charging along booms. Time ∿22 seconds. Contours from -2000 to -7000 volts in 500 volt steps.
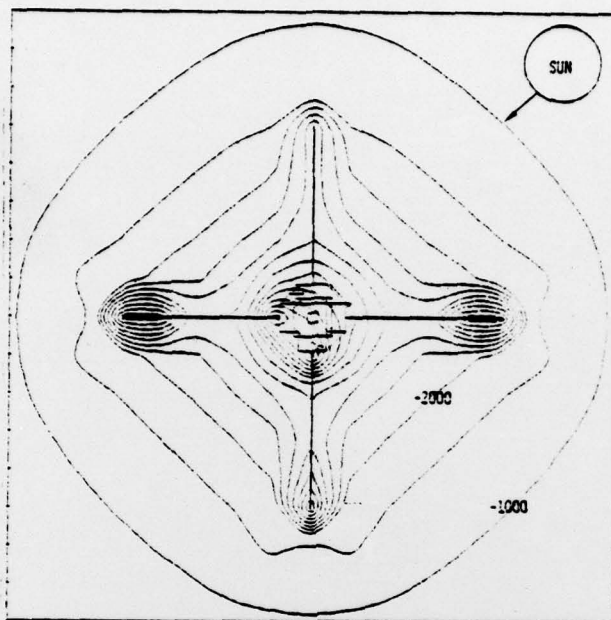
20

Figure 13. Potential contours for sunlit case in a horizontal plane through SCATHA center. Time ∿38 seconds. Contours from -1000 to -7500 volts in 500 volt steps.